

Alain Jorissen, Sophie Van Eck, Kateryna Kravchenko  
(Université Libre de Bruxelles)

Andrea Chiavassa  
(Observatoire de la Côte d'Azur, Nice)

Bertrand Plez  
(Université de Montpellier II)

Based on observations carried out with the HERMES spectrograph on the Mercator 1.2m telescope

# Tomography: I.1 technique

- **Aim** is to probe velocity fields in stellar atmospheres

Alvarez et al. (2000, A&A 362,655; 2001 A&A379, 288; 2001, A&A 379, 305)

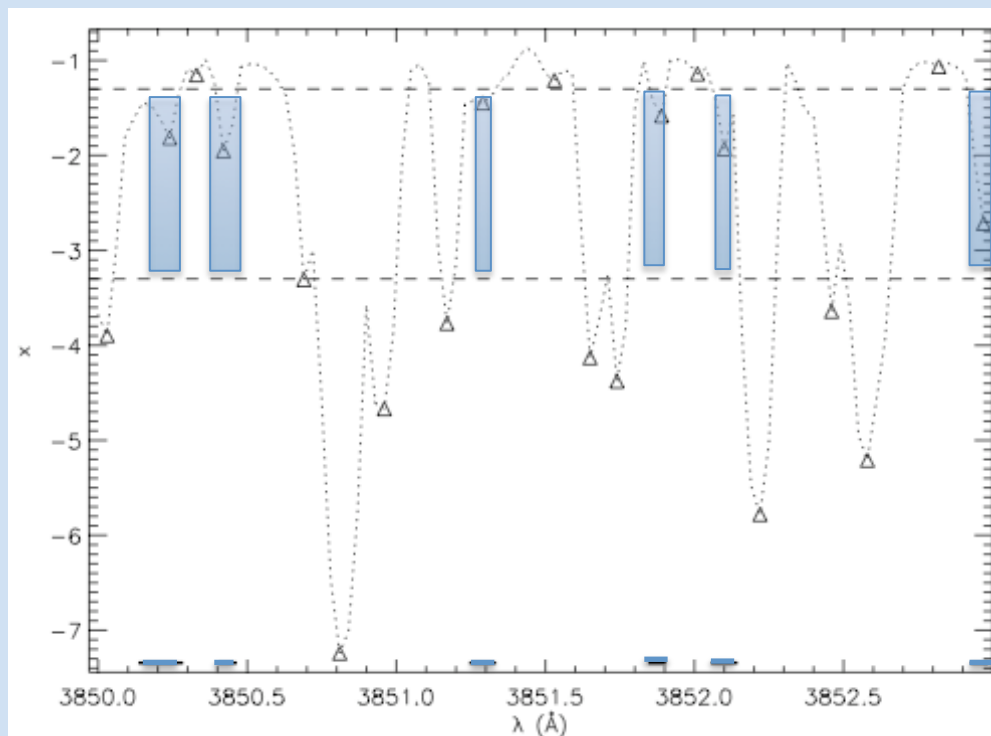
- cross-correlate the observed spectrum with numerical masks

probing layers of increasing depth

- **Construction** of the numerical masks :

Computation of the **depth function**:  $\tau_{500\text{nm}} = C(\lambda; \text{ where } \tau_\lambda = 2/3)$

$X = \log(\tau_{500})$



Region I (innermost)

Region II (middle)

Region III (outermost)

← Holes in mask II  
probing middle layer

# Tomography: 1.2 technique (improved)

Instead of imposing  $\tau_\lambda = 2/3$  for defining the mask holes,  
computation of « *contribution function* » expressing the depth of formation  
of spectral lines :

Albrow & Cottrell (1996, MNRAS 278, 337):

contribution function to the spectral-line **flux** depression:

$$C_U(\tau_0) = \int_0^1 \frac{\kappa_1}{\kappa_c + \kappa_1} (I_c - S_1) e^{-\tau/\mu} d\mu$$

with  $S_1$ ,  $I_c$ ,  $\mu$ ,  $\tau$ ,  $\kappa_1$ ,  $\kappa_c$  taken from TURBOSPECTRUM (Alvarez & Plez 1998)  
using MARCS (1D) model atmospheres.

# Tomography: I.3 technique (improved)

$S_l, I_c, \mu, \tau, \kappa_l, \kappa_c$  taken from TURBOSPECTRUM (Alvarez & Plez 1998)  
using MARCS (1D) model atmosphere:

Contribution function  $C(\lambda, \tau)$  for the Fe I  $\lambda 6546.245$  line:

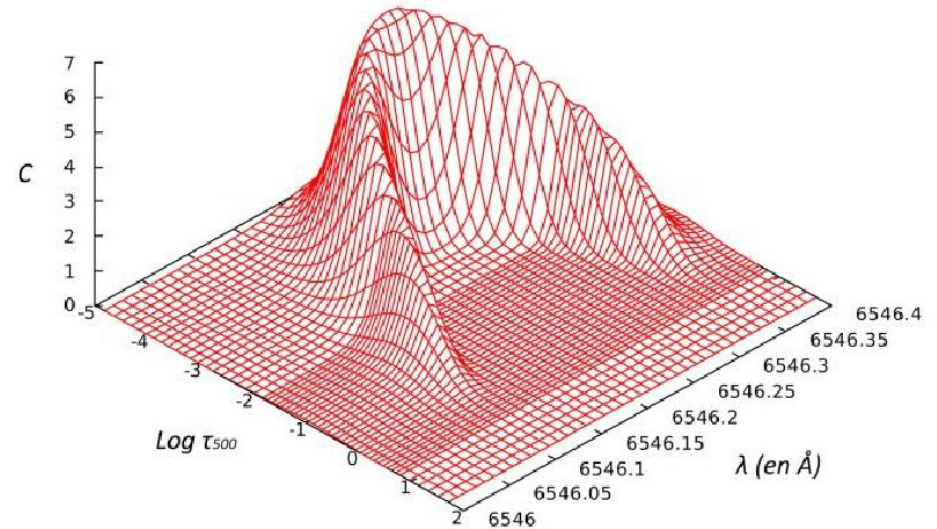
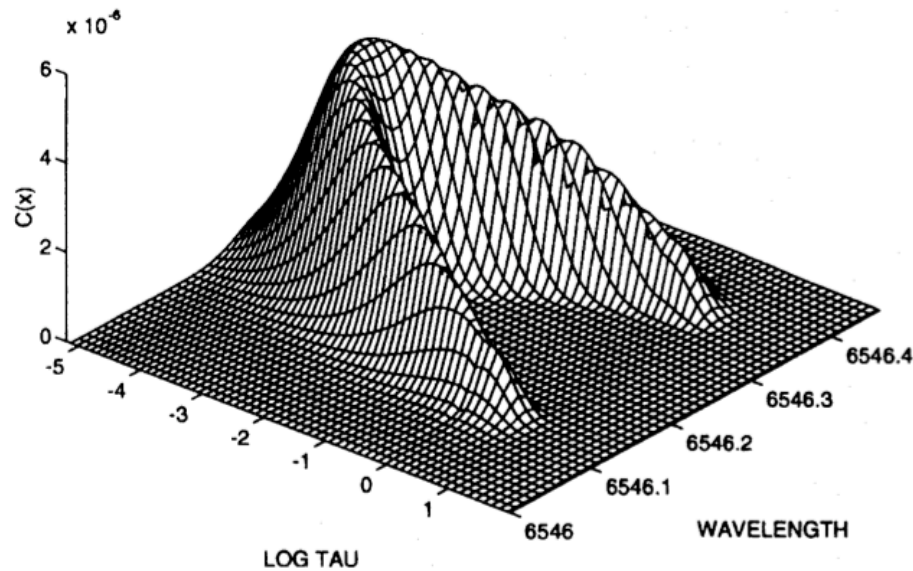


**Figure 1.** Flux contribution function for the Fe I 6546.245-Å line, with  $\log gf = -2$  and for a standard static solar abundance Kurucz model atmosphere with  $T_{\text{eff}} = 5000$  K,  $\log g = 1.0$  and  $\xi = 2$  km s<sup>-1</sup>.

Albrow & Cottrell 1996

Same spectral line, this work

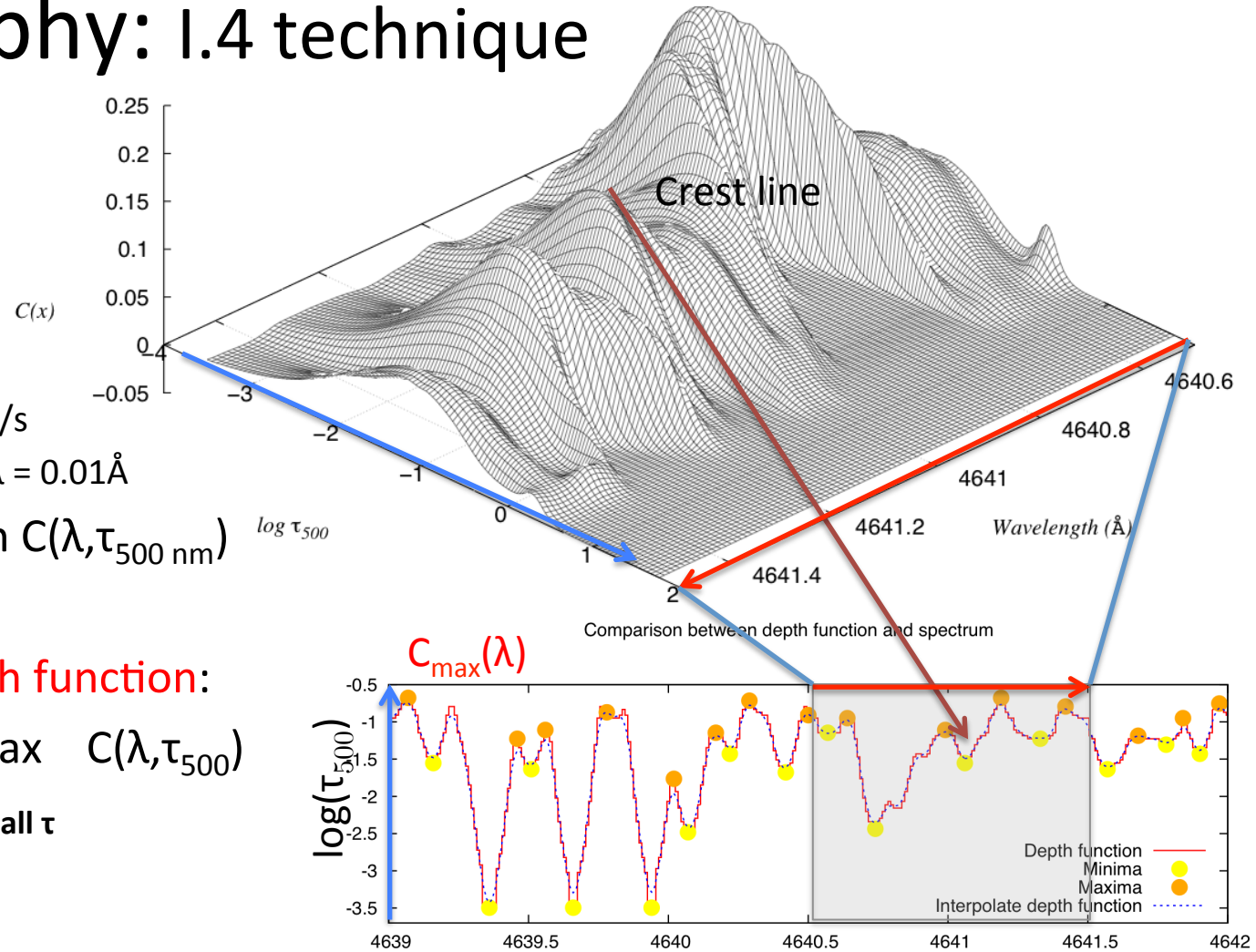
# Tomography: I.4 technique

- For RSG:
  - $T_{\text{eff}} = 3490 \text{ K}$
  - $\log g = -0.6$
  - $M = 12 M_{\odot}$
  - Solar composition
  - Microturbulence  $2 \text{ km/s}$
  - Spectral resolution:  $\Delta\lambda = 0.01 \text{ \AA}$

- Contribution function  $C(\lambda, \tau_{500 \text{ nm}})$

- Computation of **depth function**:

$$C_{\text{max}}(\lambda) = \tau_{500} \text{ of } \max C(\lambda, \tau_{500}) \text{ on all } \tau$$



Wavelength ( $\text{\AA}$ )

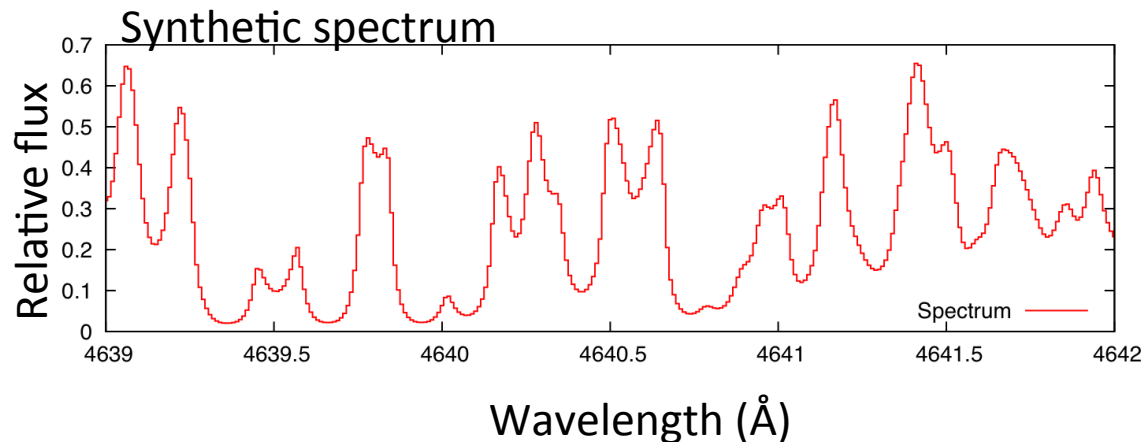
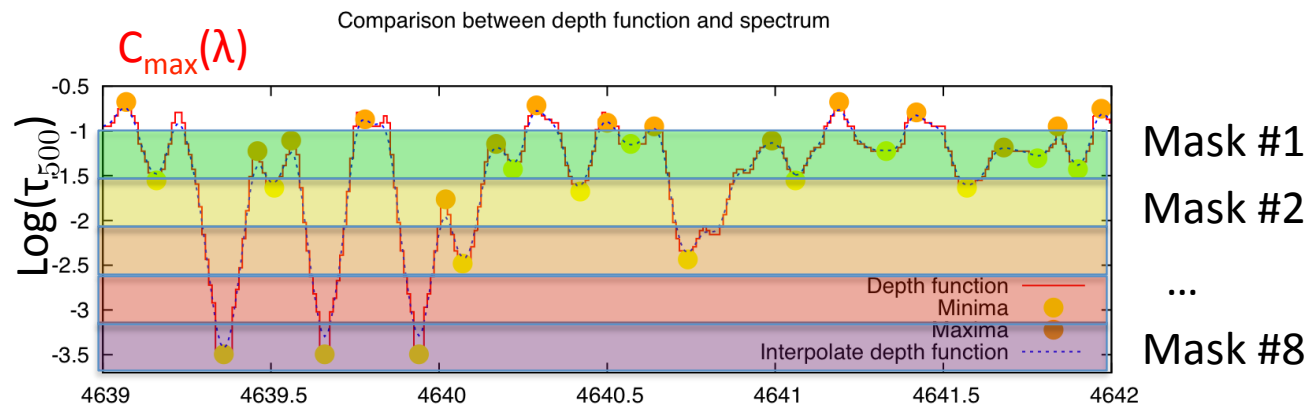
# Tomography: I.5 technique (improved)

- Computation of **depth function**:

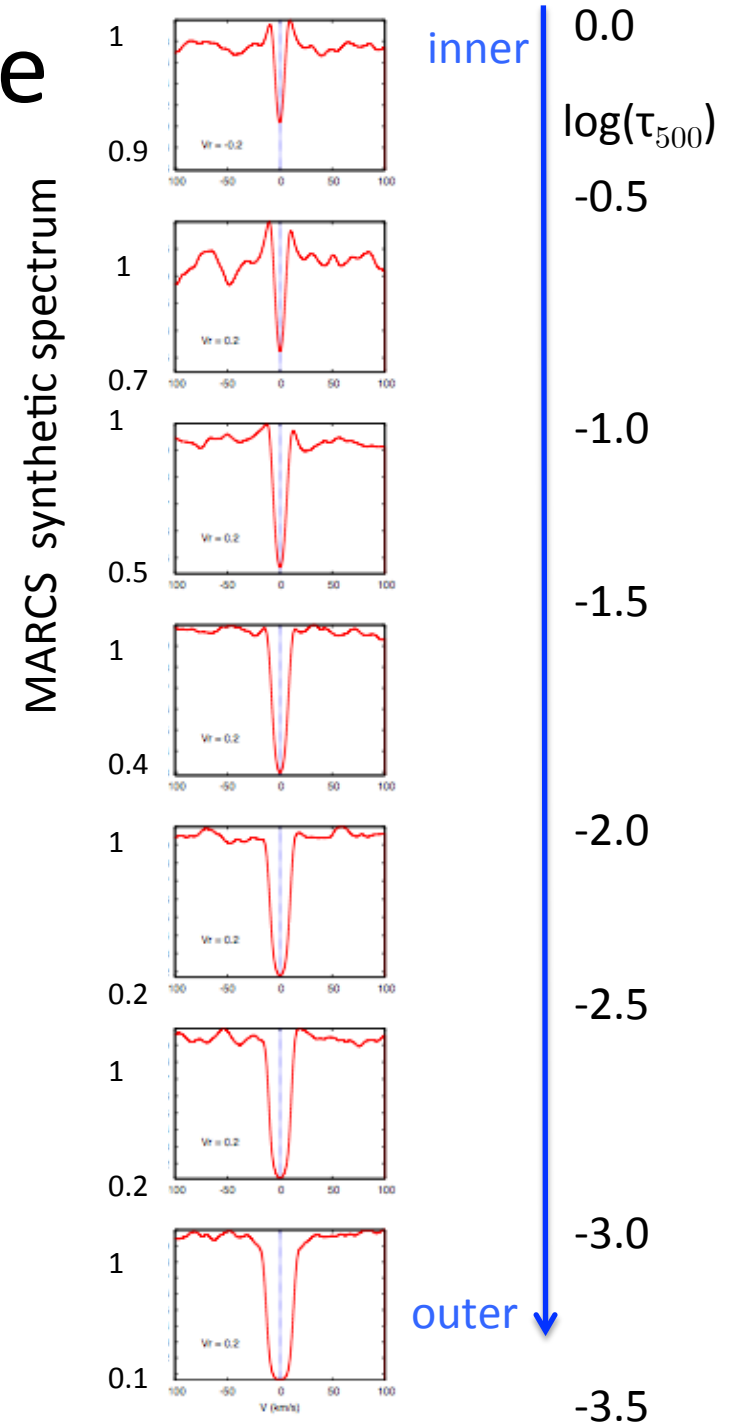
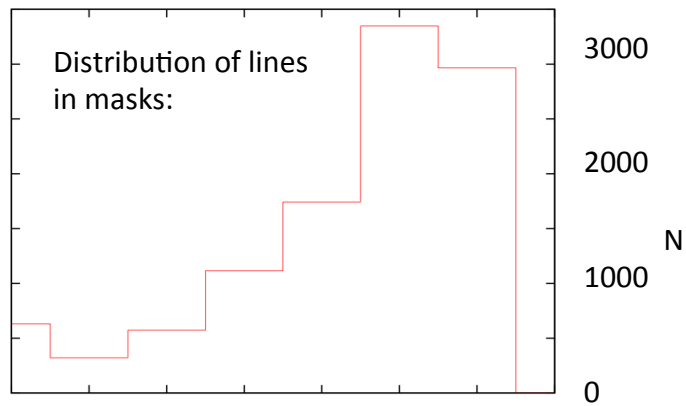
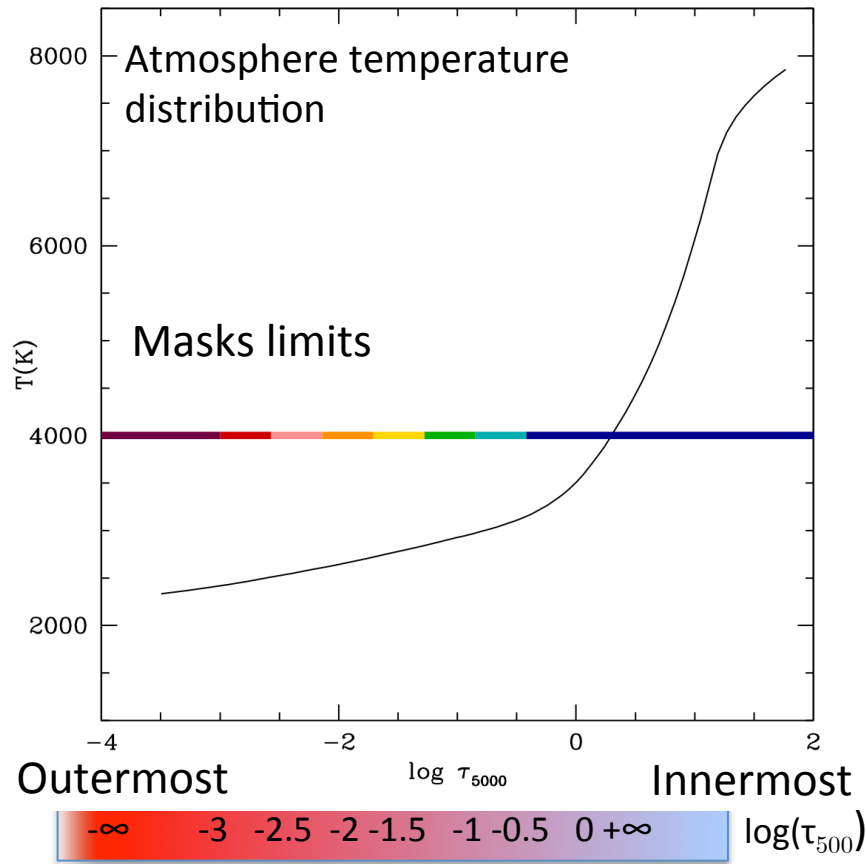
$$C_{\max}(\lambda) = \max_{\tau} C(\lambda, \tau) \quad (370 < \lambda \text{ (nm)} < 910)$$

for all  $\tau$

- Atmosphere split in 8 vertical layers
- In each layer, **mask hole** when  $C_{\max}(\lambda)$  is minimum (in  $\tau_{500}$ )



# Tomography: I.6 technique



# Tomography: II. Application to Miras

Alvarez et al. 2000, A&A 362,655

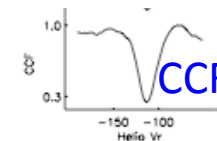
- Cross-correlation of observed spectrum with mask function  
= CCF (Cross Correlation Function)

inner

atmospheric  
depth

- Follow the progression of a shock wave in the atmosphere
  - Spatially
  - temporally

outer



time



# Tomography: III. Interpretation

Alvarez et al. 2000, A&A 362,655

## The Schwarzschild mechanism

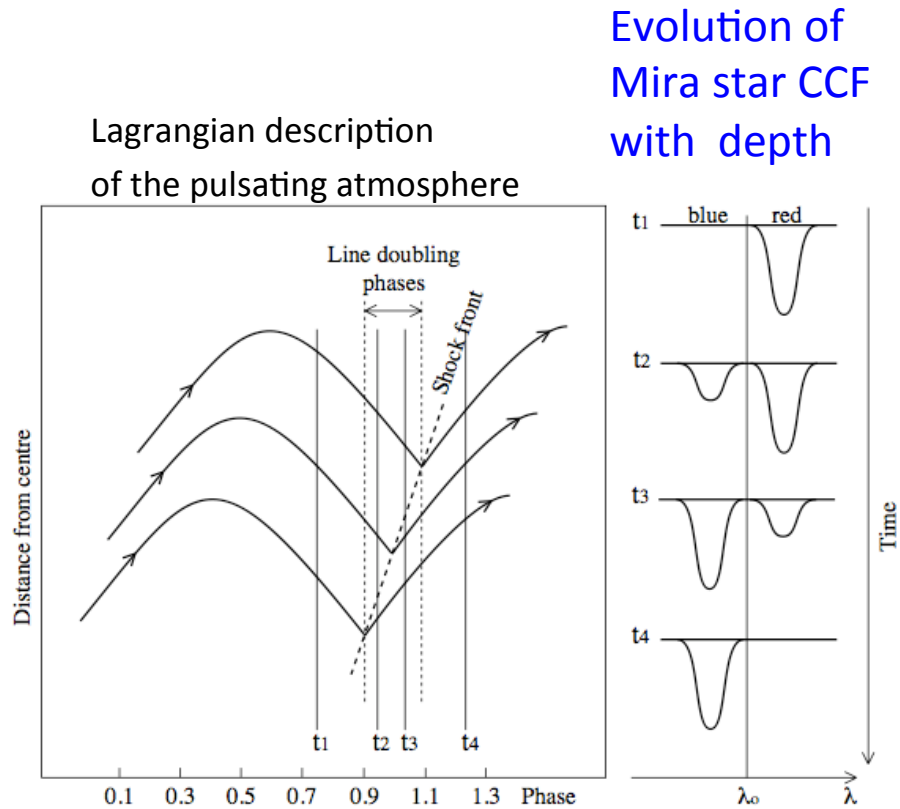


**Fig. 1.** The Schwarzschild scenario: temporal sequence followed by the intensity of the red and blue components of absorption lines close to light maximum, when the shock wave propagates through the photosphere, in the absence of any complication due to radiative processes associated with the shock wave

# Tomography: III. Interpretation

Alvarez et al. 2000, A&A 362,655

The Schwarzschild mechanism

Evolution of  
Mira star CCF  
with time at  
given depth

Lagrangian description  
of the pulsating atmosphere

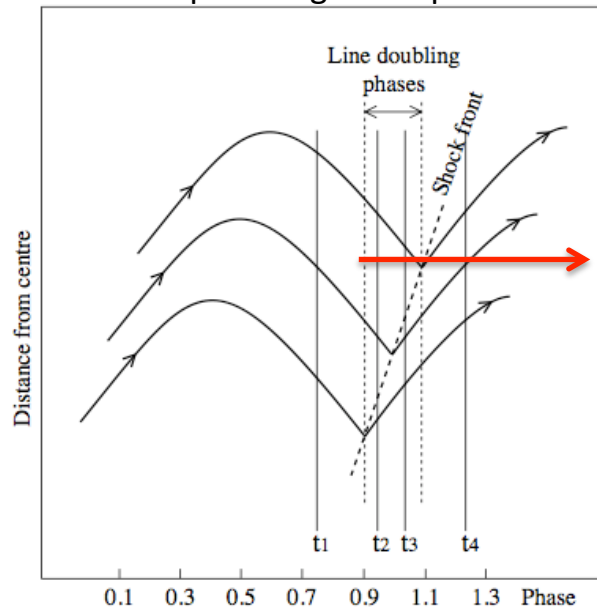
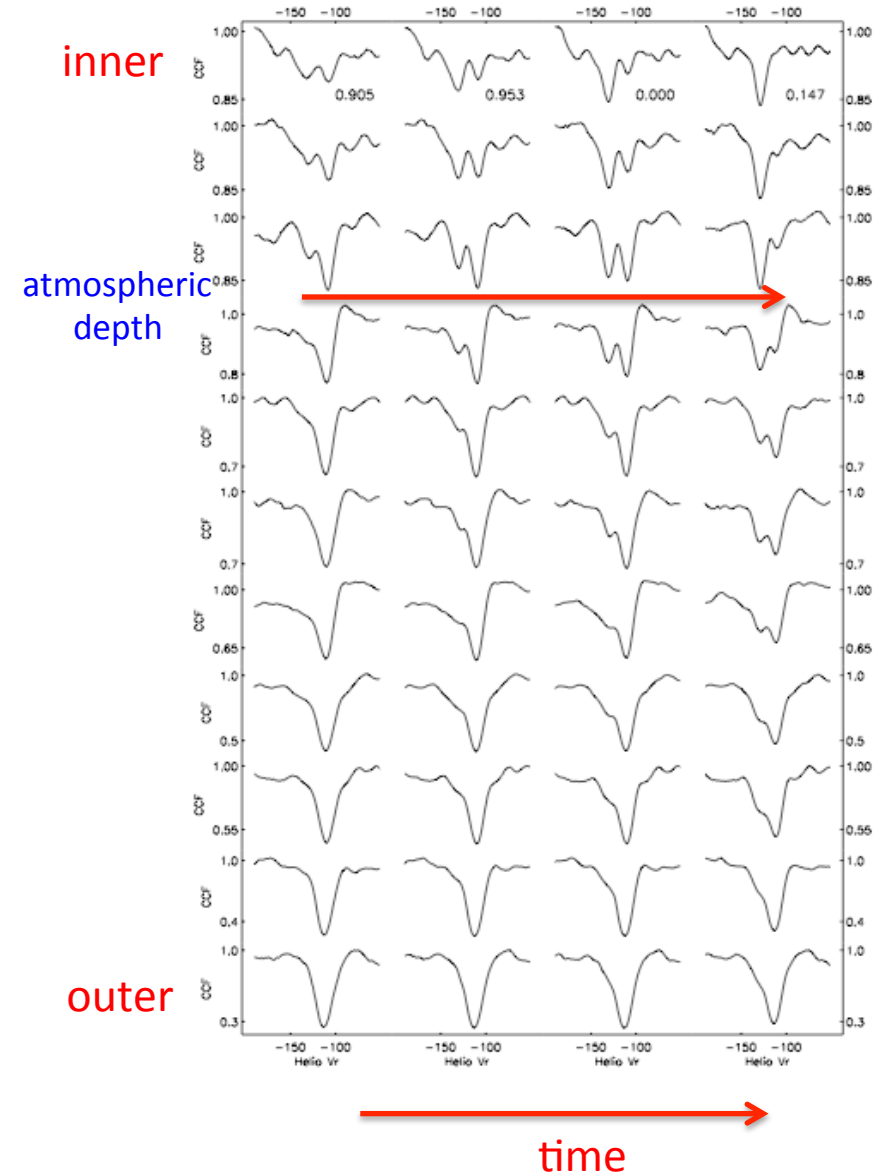


**Fig. 1.** The Schwarzschild scenario: temporal sequence followed by the intensity of the red and blue components of absorption lines close to light maximum, when the shock wave propagates through the photosphere, in the absence of any complication due to radiative processes associated with the shock wave



# Tomography: IV. Application to sg

Josselin & Plez 2007, A&A 469, 671

- Same technique and masks, applied to supergiant stars
- No cyclic behaviour
- Steep velocity gradients are observed on time scales of  $\sim 150$  days

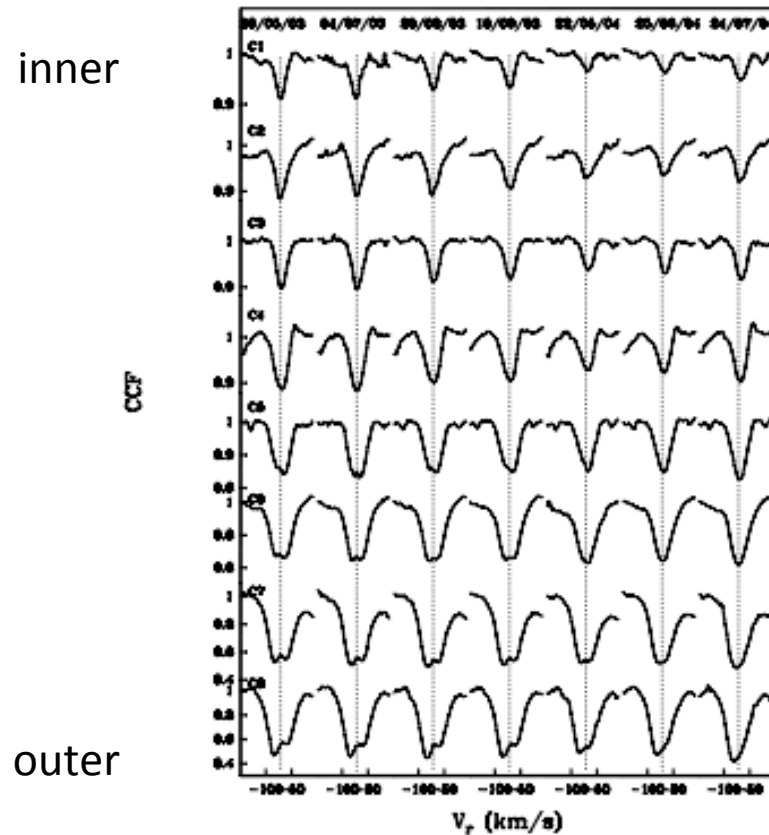


Fig. 4. CCF profiles for SW Cep. The dashed vertical lines indicate the central velocity measured in mask C1 at first epoch (upper left profile).

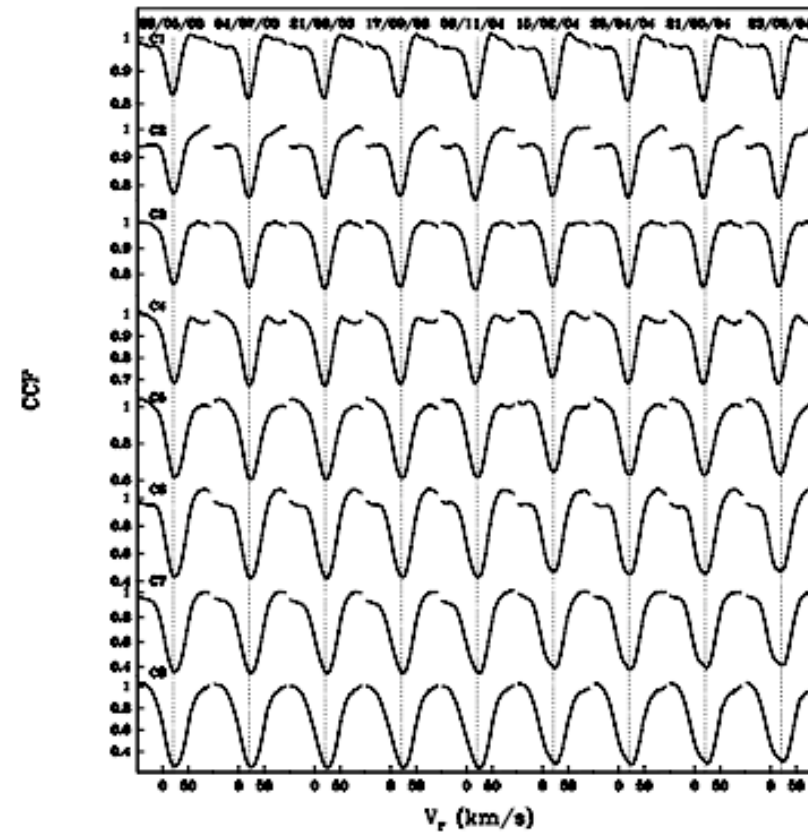


Fig. 5. Correlation profiles for  $\mu$  Cep. The vertical dashed lines indicate the central velocity measured in mask C1 at first epoch (upper left profile).

# V. Application to $\mu$ Cep

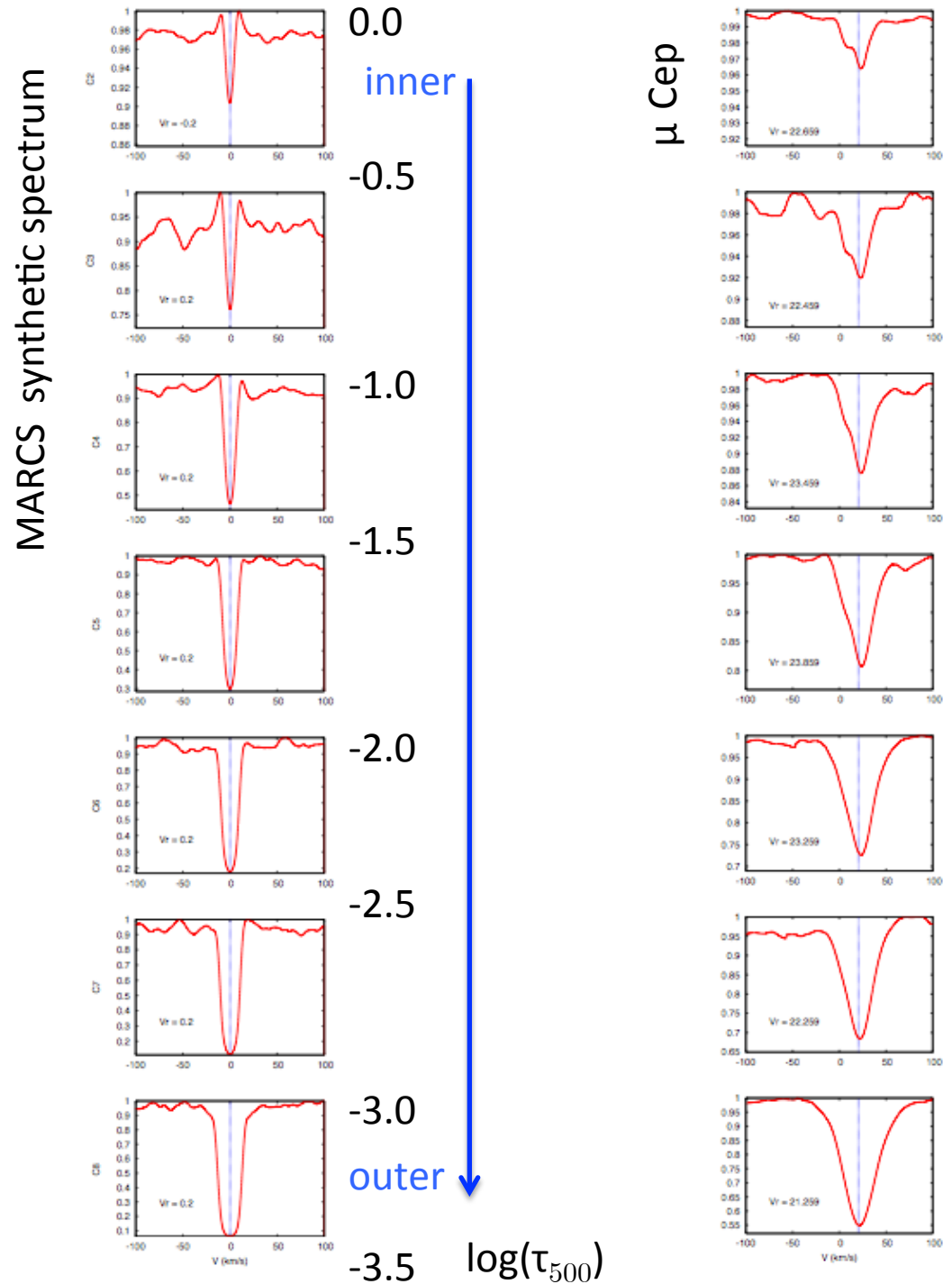


66 high-resolution  
( $R = 86\,000$ ) spectra of  $\mu$  Cep

obtained on the HERMES  
spectrograph (Raskin et al.  
2011) on MERCATOR  
telescope (La Palma)

$\Delta t = 1505$  d

Compute CCF (Radial Velocity)



---

The dance of the supergiant:

Time lapse  $\mu$  Cep

April 2011 – Jan 2015

(see the attached file  
tomo.mov)

Innermost mask

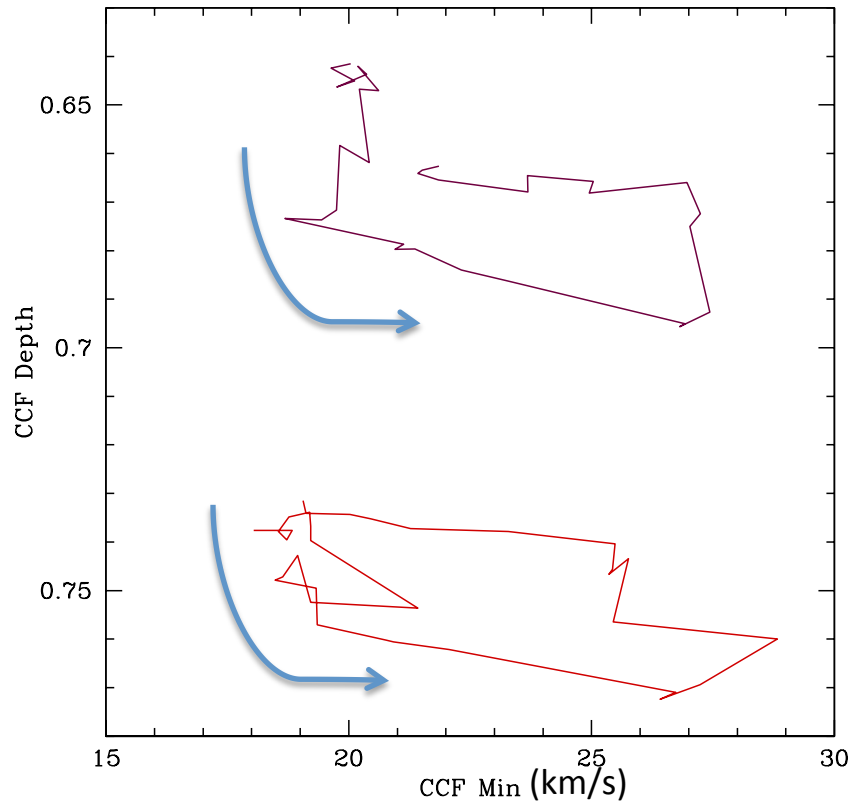
Outermost mask

$\log(\tau_{500})$

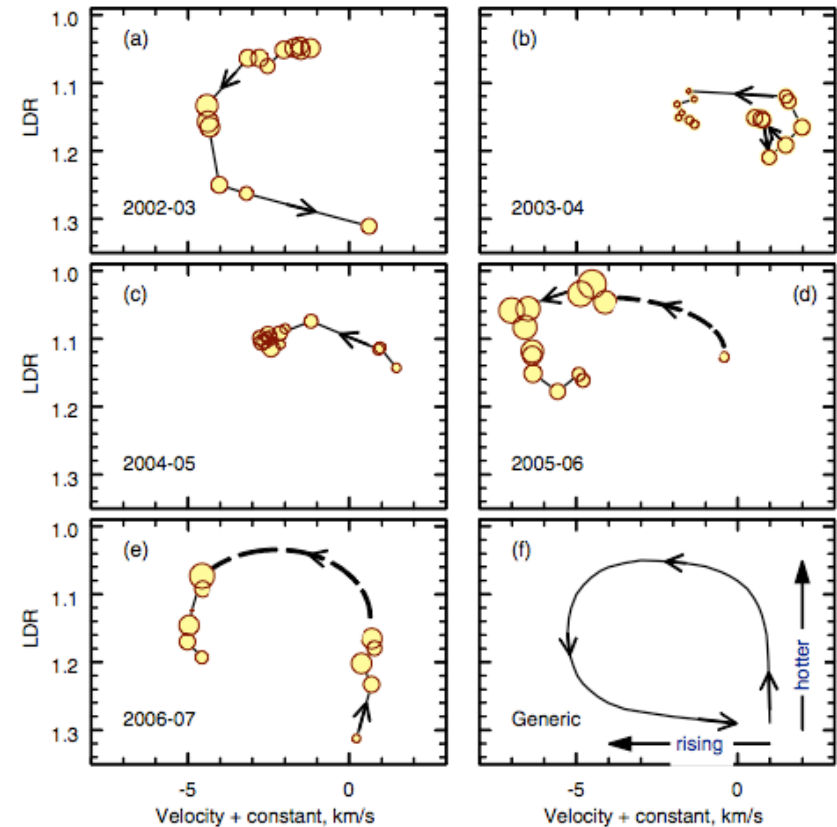
# Phase relation between velocities and line depth (ratio)

Hysteresis (caused by convective cells?)

$$\text{LDR} = \text{Line Depth(VI)} / \text{Line Depth(Fel)}$$



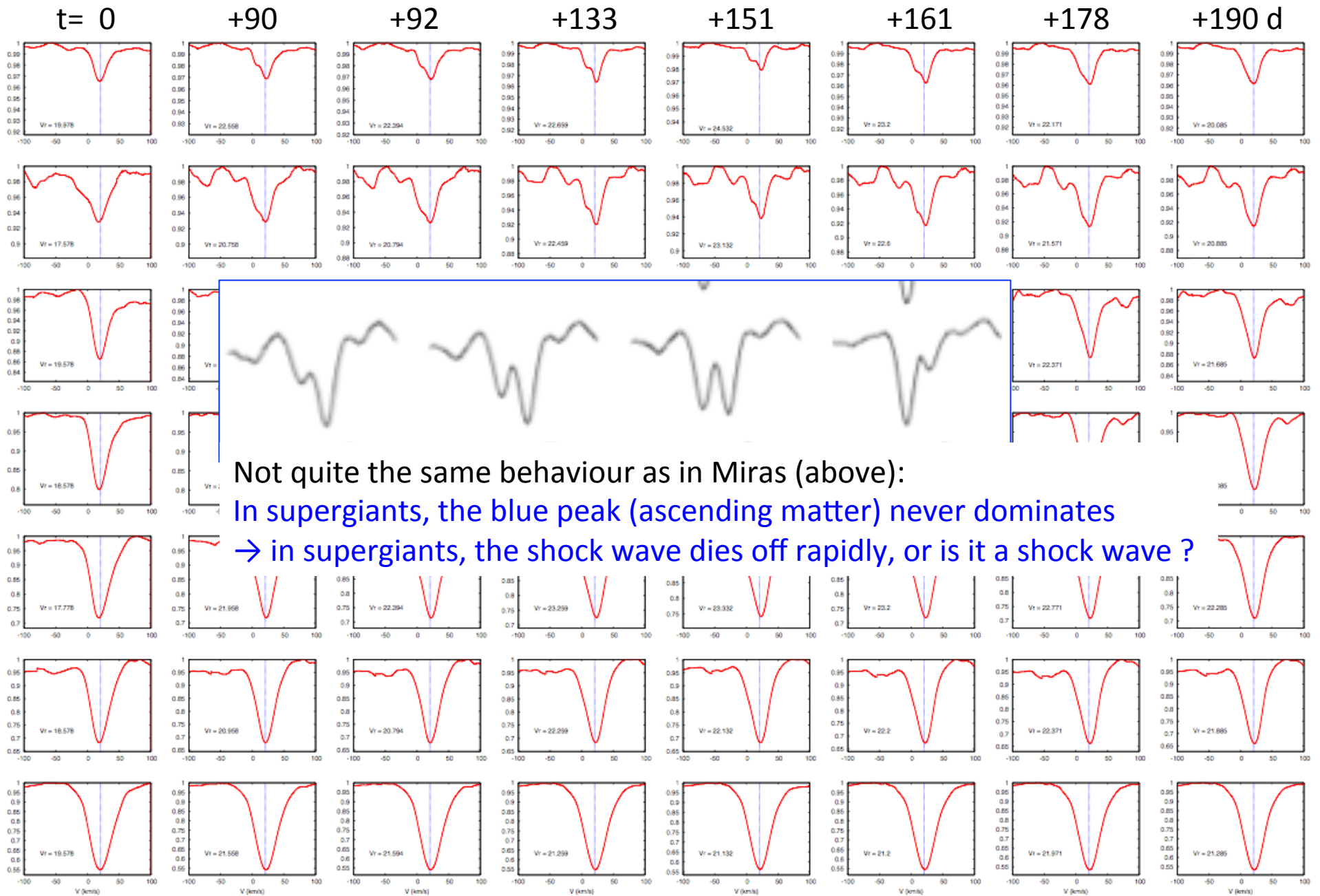
$\mu$  Cep  
Observation: 550 d



Gray, 2008, AJ 135, 1450

Betelgeuse

Typical time 400 d



# Another example, 450 d later

t= 0

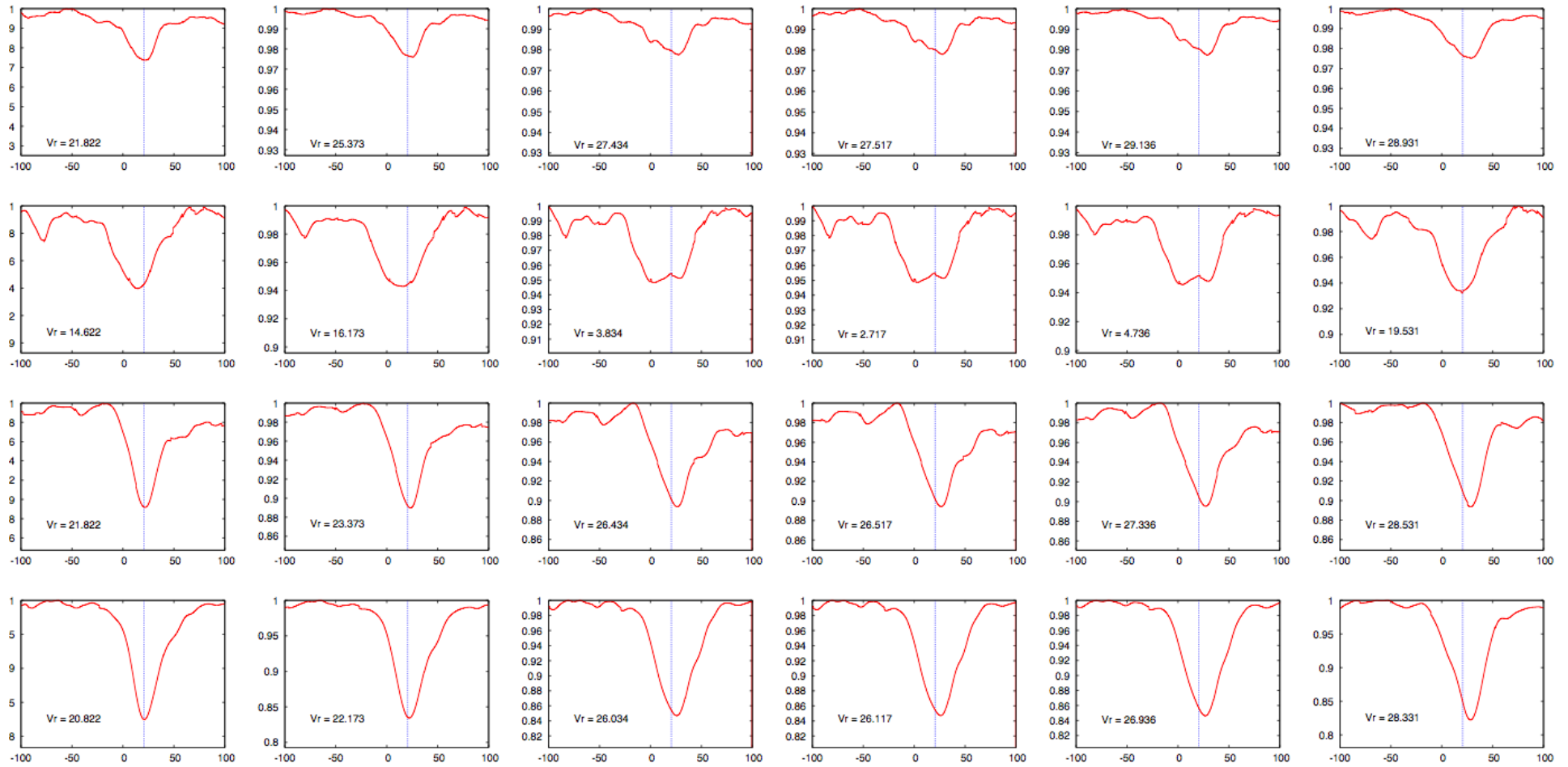
+18

+65

+67

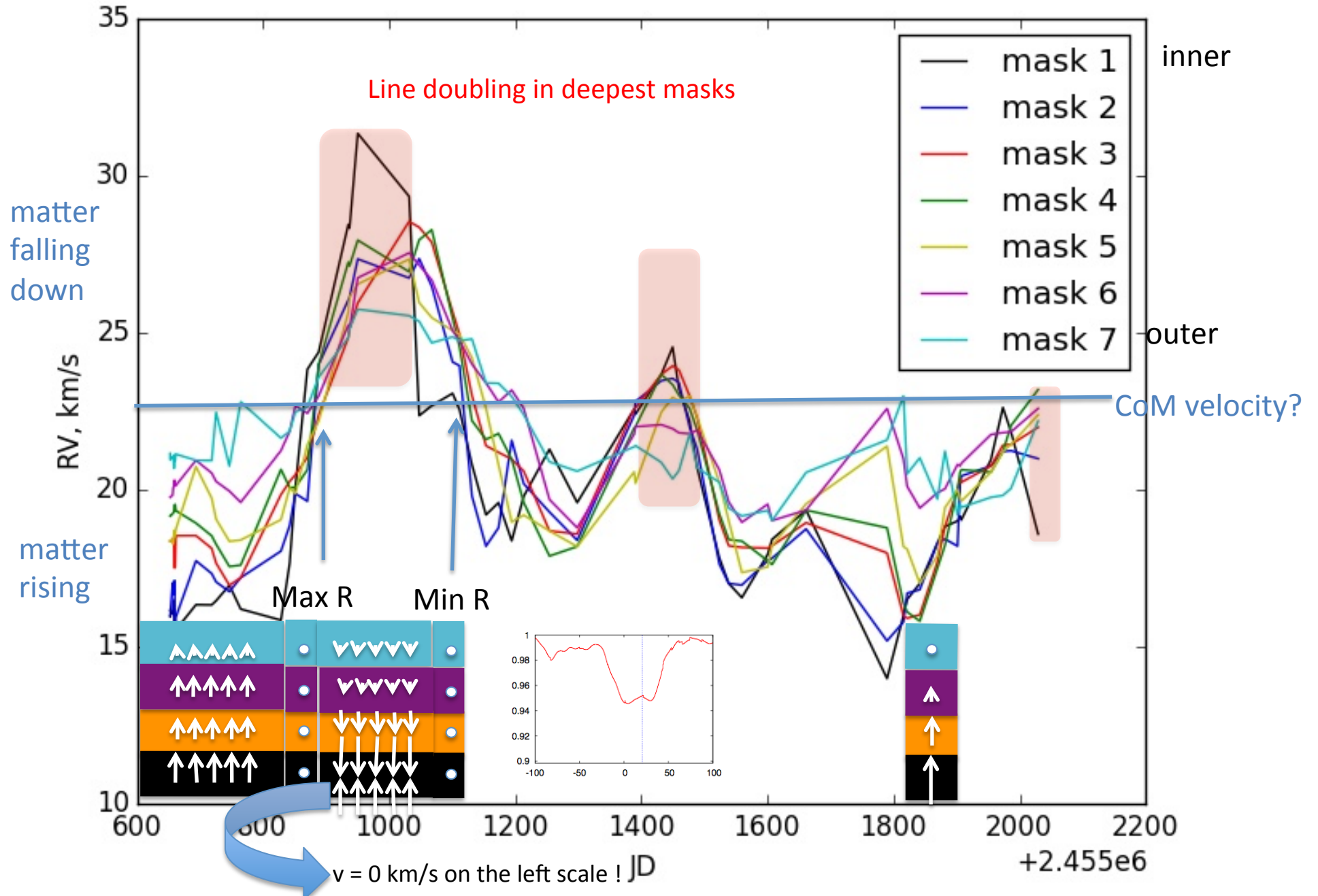
+80

+161 d

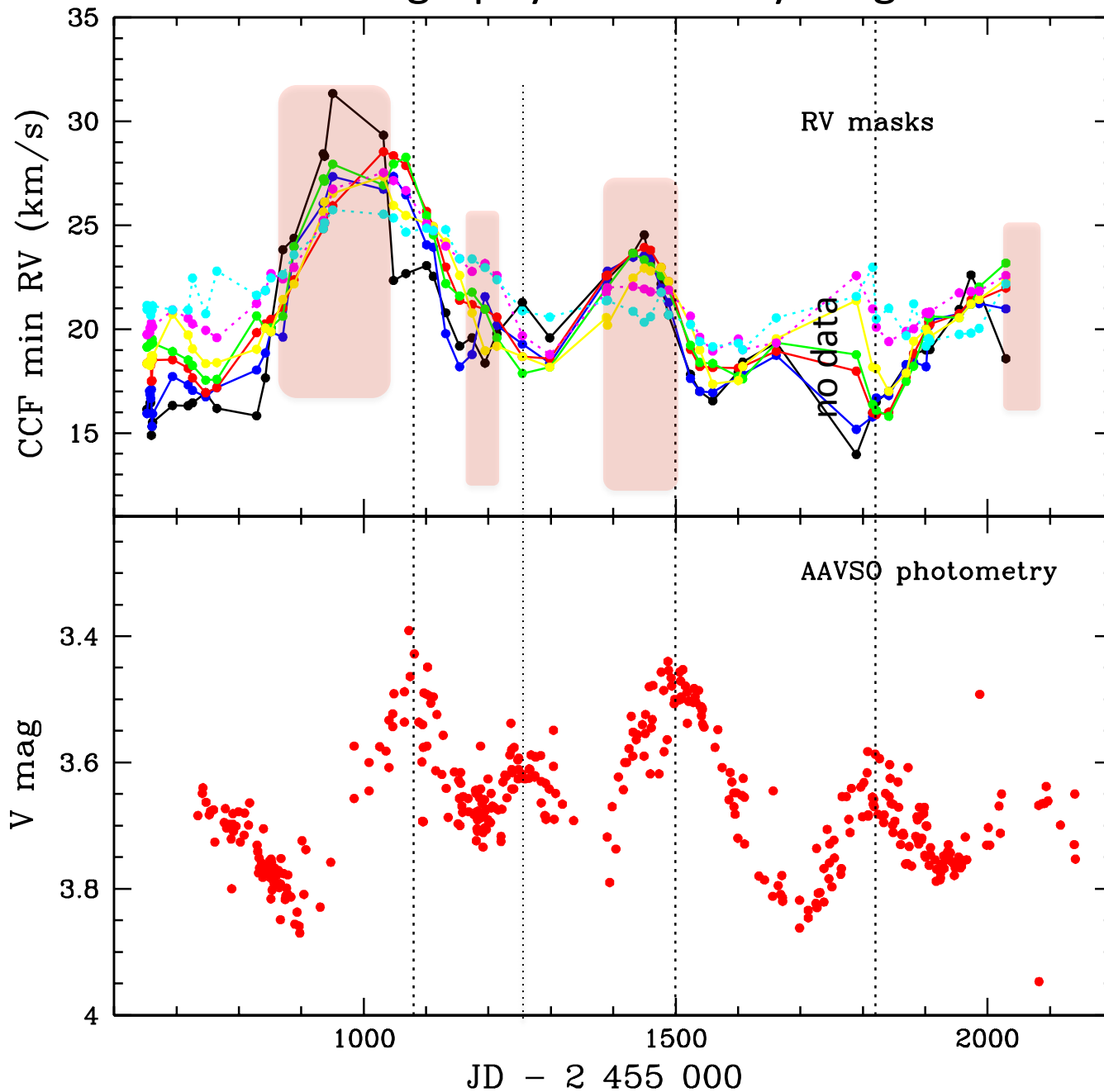




# Tomography: V. Velocity curve of $\mu$ Cep



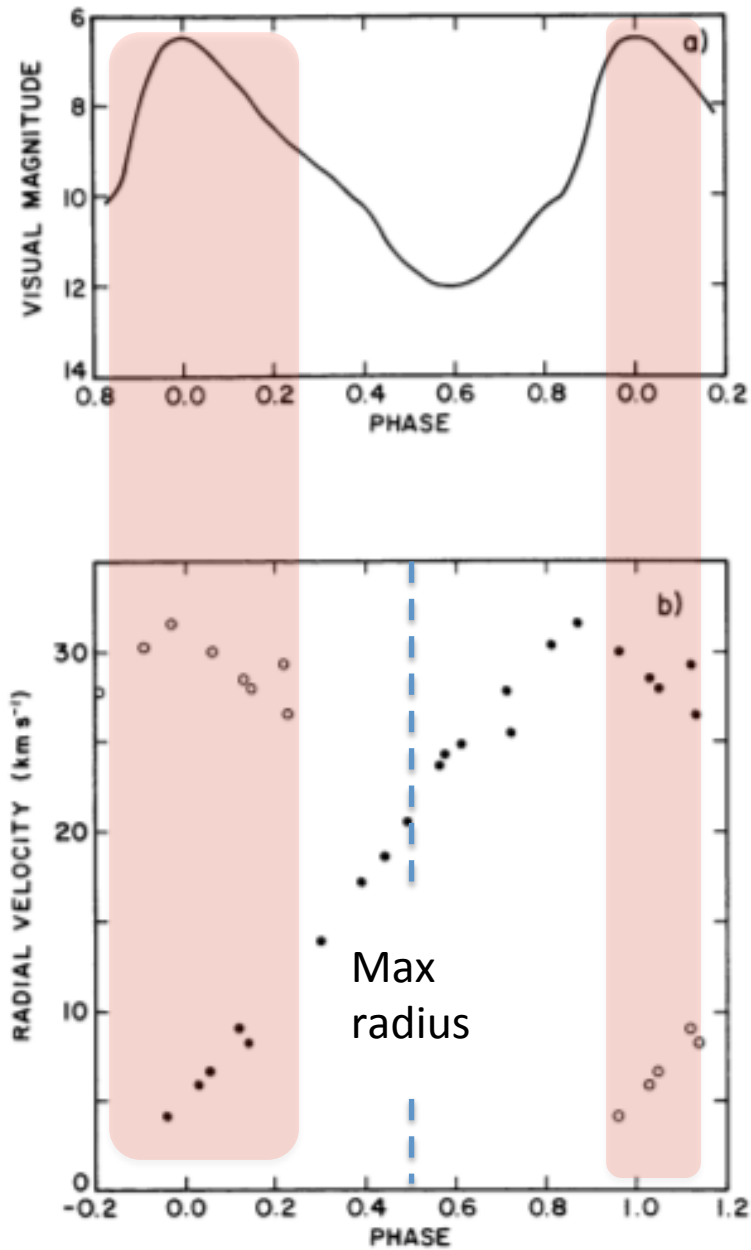
# Tomography: V. Velocity & light curves of $\mu$ Cep



Line doubling in deepest masks

occurs during the rising part of the light curve

# Tomography: VI. Situation in Mira variables (R Cas)



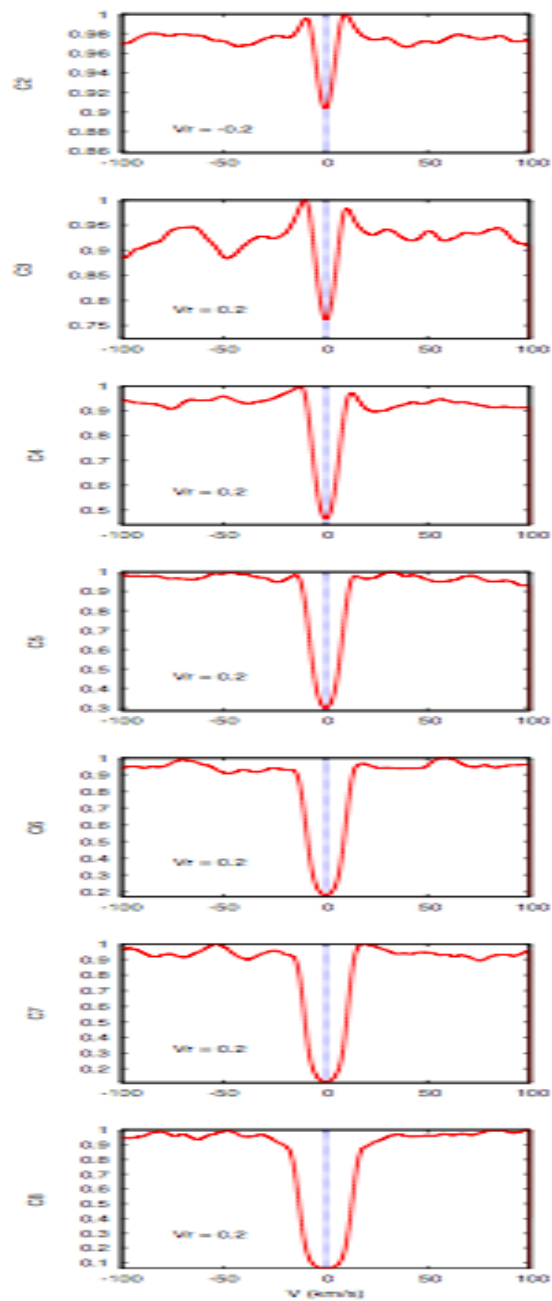
Line doubling around max light

receding

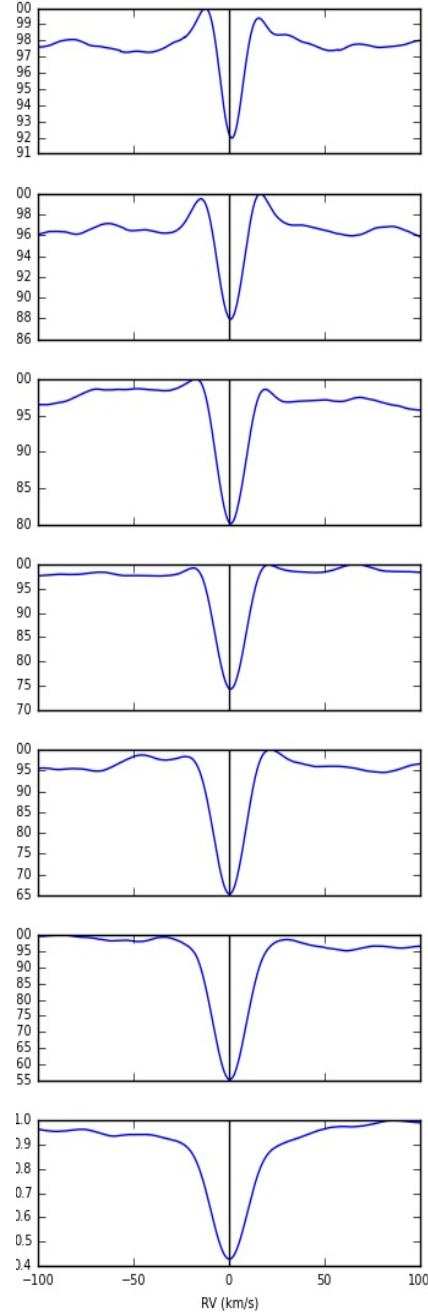
CO  $\Delta v = 3$  lines

approaching

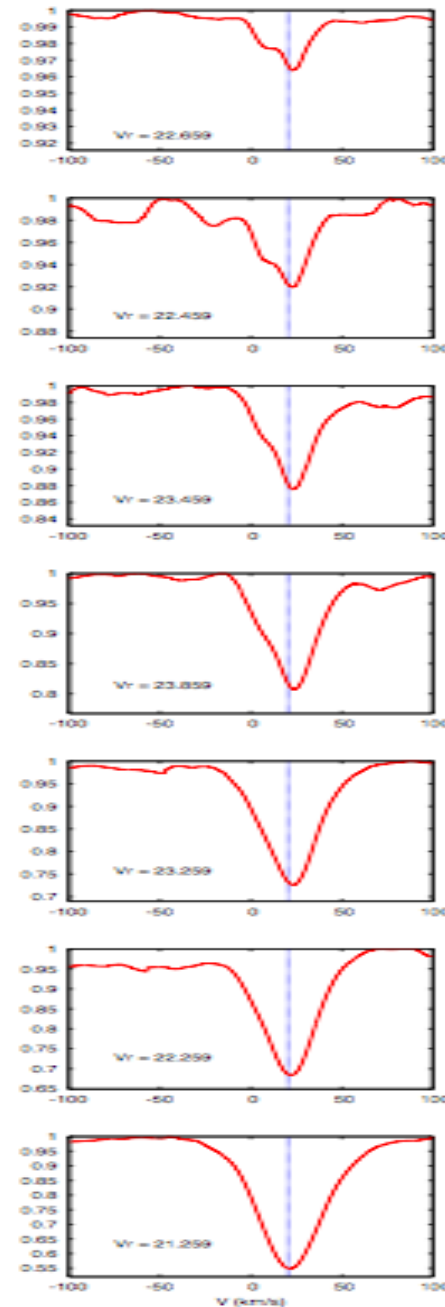
Synthetic MARCS 1D



Synthetic CO<sup>5</sup>BOLD 3D

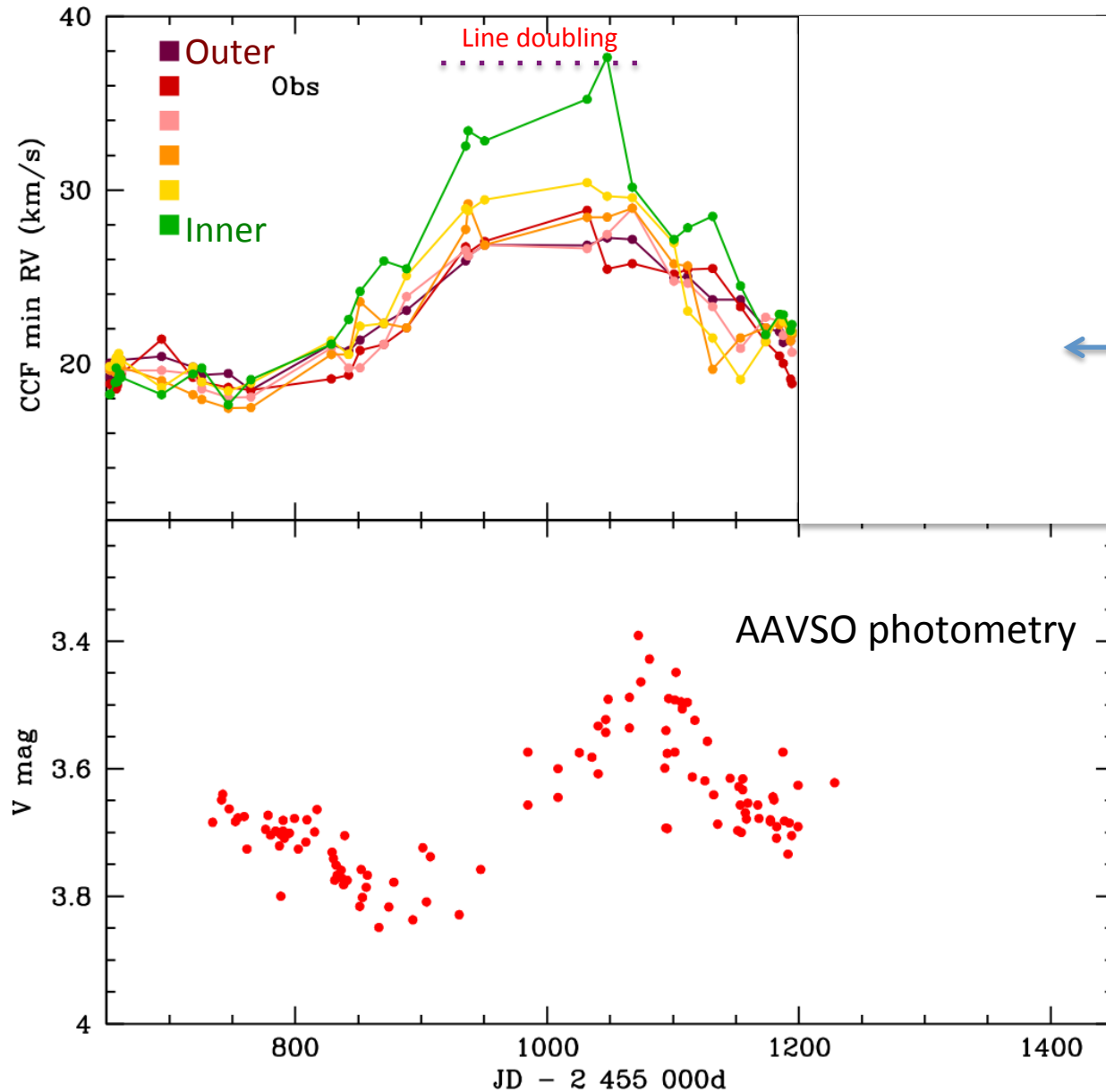


Observed  $\mu$  Cep



Tomography:  
VII. Comparison  
with  
3D models

# Tomography: VII. Comparison with 3D models



All masks show consistent variations following radial-velocity curve

## 3D spectra:

4 OPTIM3D snapshots from CO<sup>5</sup>BOLD 3D models (Chiavassa et al. 2011, A&A 535, A22)

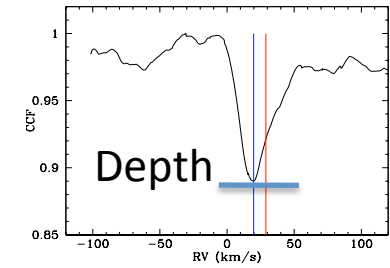
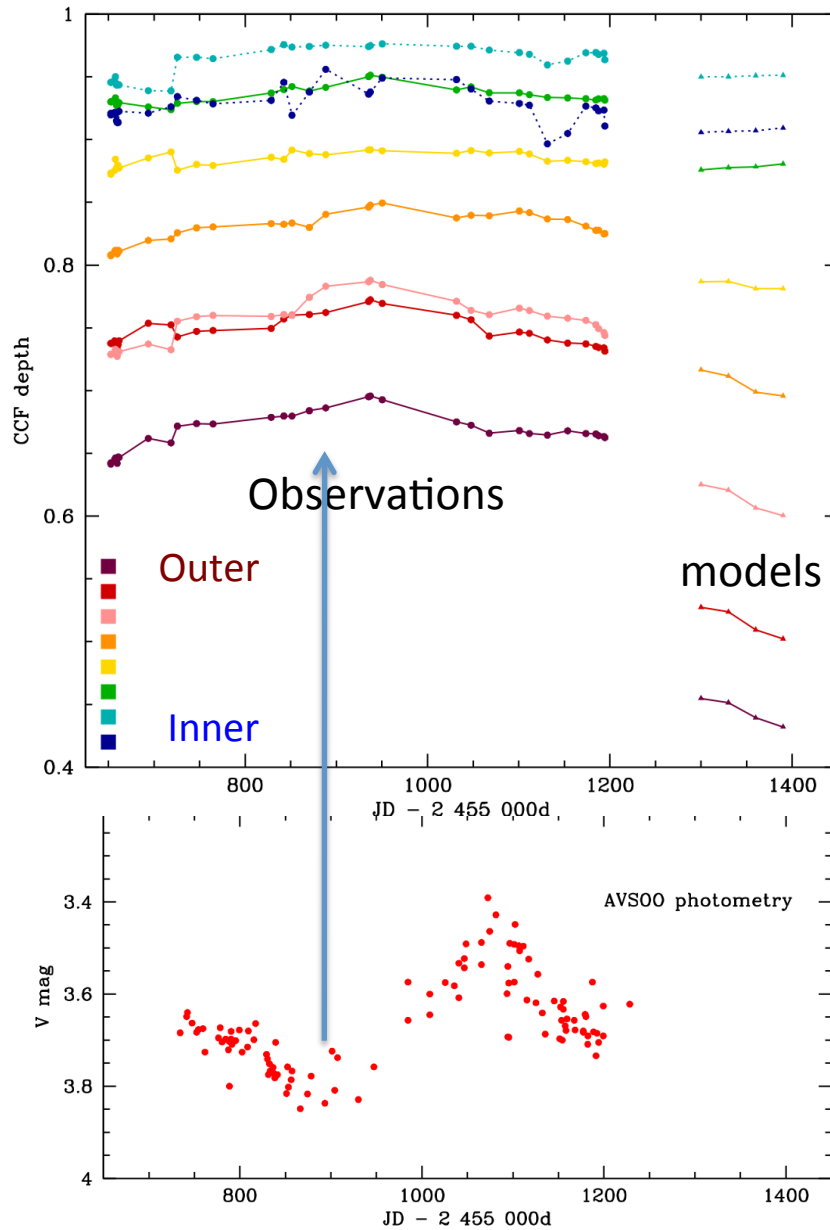
$T_{\text{eff}} = 3430 \text{ K}$

$M = 12 M_{\odot}$

$R = 846 R_{\odot}$

$\log g = -0.35$

# CCF depth



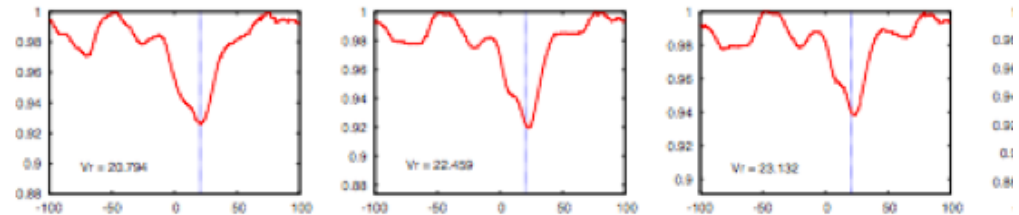
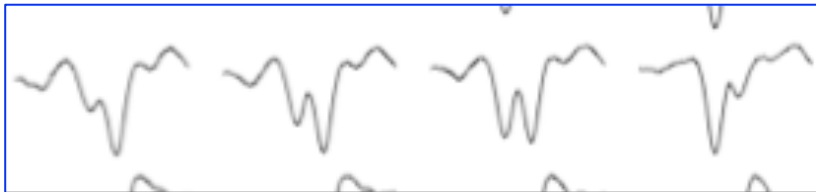
Inner masks sample weak lines  
Outer masks sample strong lines

Comparison with 3D CO<sup>5</sup>BOLD  
(4 snapshots):  
for outer masks especially:  
3D CO<sup>5</sup>BOLD lines are deeper  
(factor ~1.5 to 2)

# Summary

## OBSERVED FEATURES:

- In the supergiant  $\mu$  Cep, line doubling *systematically* occurs
  - on the rising part of the light curve;
  - in the innermost masks;
  - is never seen in the outermost masks;
  - with the red component stronger.
- Hysteresis between CCF/line depth and velocity
- The evolution of line doubling is different in Miras and supergiants



## COMPARISON WITH 3D MODELS:

Some discrepancies for line depths, widths, & velocities ( $\tau$ )

currently being investigated by increasing numerical resolution of models (Chiavassa et al.)

A close collaboration with 3D-modellers is needed to make the models reproduce all these data